JOURNAL OF GEOPHYSICAL RESEARCH, VOL. 96, SUPPLEMENT, PAGES 3307–3322, FEBRUARY 28, 1991

Effect of Low-Latitude Western Boundary Gaps on the Reflection of Equatorial Motions

YVES DU PENHOAT

Groupe SURTROPAC,
Institut Français de Recherche Scientifique
Pour le Développement en Coopération (ORSTOM),
Nouméa, New Caledonia

MARK A. CANE

Lamont-Doherty Geological Observatory of Columbia University,
Palisades, New York

The western tropical Pacific is thought to be an important zone for generating El Niño: reflections at the boundary make it a source region of equatorial Kelvin waves. Calculations of the effect of a gappy western boundary on the reflection process are carried out in the framework of the low-frequency limit of the shallow-water equations and thus are highly idealized. The method is also applied to a schematic version of the flow through the Indonesian seas from the western Pacific to the Indian Oceans. The results indicate some strong sensitivities to the location of the gap and to the structure of the incoming flows. In addition, the results can be quite different, depending on whether the zonal extend of the gap is assumed to be infinite or finite. (More precisely, the latter means that the extend of the gap is short compared with the zonal wavelength of the relevant free waves at that frequency.) In view of the complexity of the results for even such a simplified model, it will be very difficult to be confident of any modeling study of the Indonesian throughflow short of a highly resolved numerical calculation with a detailed representation of the geometry and bathymetry. Nonetheless, we offer tentative conclusions concerning the efficiency of the western Pacific boundary as a reflector. Our results suggest that the realistic boundary will not greatly alter expectations based on a simple solid boundary if the reflections important for El Niño are primarily in motion, represented by low-order Rossby modes. This is also consistent with observational evidence indicating no anomalous throughflow during El Niño events.

1. INTRODUCTION

Recent studies have made heavy use of linear equatorial wave concepts to understand the recurrence of El Niño Southern Oscillation (ENSO) events. For all their complexity, even coupled general circulation models have been interpreted in terms of linear wave concepts. The western tropical Pacific is thought to be an important area for generating El Niño: reflections at the boundary make it a source region of equatorial Kelvin waves, and it also contains a large pool of warm water that could be an important part of an El Niño event when advected by unusual eastward flow (see *Zebiak and Cane*, [1987], among others).

White et al. [1985], studying the increase of heat content, claimed that extratropical Rossby waves generated by anomalous wind curl, after impinging on the western Pacific coasts, could generate an equatorial Kelvin wave, which in turn would trigger an El Niño event. However, *Harrison et al.* [1989], in numerical model experiments forced with different observed wind sets, strongly suggest that the 1982 - 1983 El Niño event was a result of wind forcing in the equatorial wave guide. *Graham and White* [1988] emphasized a necessary role for off-equatorial Rossby wave perturbations in maintaining the oscillatory nature of El Niño cycle. *Battisti* [1988, 1989] tempers their conclusions, finding that off-equatorial (poleward of 6° from the equator) Rossby waves could not be involved as a triggering mechanism for an ENSO event in his model. Nonetheless, he also points to the importance of western boundary reflections for both event initiation and termination, but focuses on the more equatorially confined modes. *Zebiak* [1989], studying heat content variability in the context of a linear, dynamical model, discusses the role of Rossby waves and western boundary reflections: some of the equatorial zonal transport near the western boundary originates at higher latitude in the interior of the basin, owing to the structure of Rossby wave - induced circulation, but the zonal convergence/divergence at the western boundary near the equator largely determines the reflected Kelvin wave signal.

Whether or not extratropical influences are important depends on how well the western boundary can reflect disturbances into equatorial Kelvin waves. In both oceanic and coupled models, reflections of Rossby waves on the western boundary are the basic mechanism to overcome the positive feedback tending to raise sea level at the east. In most models, the western Pacific boundary is a nice smooth wall, but, in reality, it consists of irregular island chains. Therefore it could be a poor wave reflector, allowing Rossby waves to pass through its many passages.

There have been a few attempts to quantify the flow through the Indonesian archipelago. All studies agree that a flux exists from the Pacific to the Indian Ocean, but estimates of its magnitude vary over a broad range. *Wyrtki* [1961] deduced a 2 - Sv flow in the upper 200 m, calculated from sea level. *Murray and Arief* [1988] made an attempt to directly measure the flow through the Lombok Strait (between Bali and Lombok islands at 8°27'S). They described a distinct seasonal transport from 1 to 4 Sv in northern summer months. They consider that the Lombok Strait transport represents 20% of the total transport between the Pacific and Indian Oceans (the main passage would be along Timor Island). On the basis of freshwater and mass balance, *Piola and Gordon* [1984] have found that a 10- to 14-Sv transport through the Indonesian archipelago is required. *Wyrtki* [1987] inferred the through flow from the pressure gradient between the two oceans. He found a clearly defined seasonal cycle, strongest in July - August and weakest in January - February, in agreement with *Murray and Arief* [1988]. However, the interannual variability of the pressure gradient is not clearly linked with

Paper number 90JC01798.
0148-0227/91/90JC-01798$05.00

ENSO recurrences: sea level on both sides of the archipelego is low during ENSO events. Recently, the western Pacific has been the scene of intensive investigations (i.e., the Western Equatorial Pacific Ocean Circulation Study (WEPOCS) experiment; *Lindstrom et al.* [1987]. *Lukas* [1988] has investigated the interannual variability of the Mindanao boundary current (at 6°N), as inferred from sea level measurements, and has concluded that there is no clear relationship between the flux of the Mindanao current and the strength of an ENSO signal. This does not support the hypotheses of *White et al.* [1985] about the role of extraequatorial Rossby wave reflections at the coast of Asia.

Our motivation for this work was to know how efficient the Pacific western boundary is at generating equatorial Kelvin waves by the reflection of mass flux incidents at the boundary. How much is lost in jumping the entrance of the Indonesian archipelago? Does the irregular, porous western boundary support the simple planetary wave reflections which occur in numerical models?

We focus this investigation of the effect of leaky boundaries on basinwide adjustment processes, rather than on the details of boundary layers in the vicinity of coasts or gaps. Our approach uses extensively the techniques and results of *Cane and Sarachik* [1976, 1977, 1981] (henceforth referred to as CS I, CS II, and CS III, respectively), and is an extension of *Cane and du Penhoat* [1982] and *du Penhoat et al.* [1983]. We work within the framework of the linear shallow-water equations and solve for the asymptotic flows which result when a source is switched on at $t = 0$ and remains steady thereafter. The results of this canonical problem are characteristic of all low-frequency flows.

We solve in section 2 the problem of Rossby waves impinging on a coast with a gap. We check the result for an infinitesimally thin coast against that for a coast of finite width. In section 3, the effect of a more general incoming flow with a delta function form is investigated. Section 4 contains a calculation for the Pacific western boundary, and section 5 summarizes our conclusions.

2. Rossby Wave Motion on a Western Boundary With a Gap

In what follows, all variables have been nondimensionalized, using the usual equatorial scaling (e.g., CS I). The formal problem considered here is the following: At $t = 0$, a flow comprised of Rossby waves impinges on a western boundary at $x = 0$. The flow has the form $H(t)$, a step function in time: it is zero for $t < 0$ and unchanging thereafter. The coast is oriented north - south, extending from $-\infty$ to b and from a to $+\infty$, thus presenting a gap of width $d = a - b$. We are interested in low-frequency motion for which frequency is small compared to the equatorial scaling frequency, and seek the asymptotic response as $t \to \infty$.

CS I have shown that for large t, the asymptotic motions are of three kinds: (1) Long eastward propagating Kelvin waves, with zonal velocity u and height h proportional to ψ_0, the zeroth order Hermite function: $\psi_0 = \pi^{-1/4}\exp(-\frac{1}{2}y^2)$. The large t response is steady for an $H(t)$ time dependence and is independent of x. (2) Long Rossby waves, propagating energy westward. Both the equatorial Kelvin wave and the long Rossby waves satisfy the meridional geostrophic relation

$$yu + \frac{\partial h}{\partial y} = 0 \qquad (1a)$$

The equatorial Kelvin wave has meridional velocity $v = 0$ and the long Rossby waves have $v \approx 0$. Again, the large t asymptotic form is independent of t and x. (3) Short Rossby waves (including the mixed Rossby-gravity wave); the sum of such modes is an ever-thinning boundary layer trapped to $x = 0$ (see CS II); their group velocity is so small that even a small amount of friction prevents them from propagating. They are trapped to the western boundary, where they form a boundary current. It may be shown (CS II, p. 404) that at $x = 0$ this current has the form $u^B = -\partial\chi/\partial y$, $V^B = \partial\chi/\partial\chi$, $h^B = y\chi$, where χ is a stream function for the boundary layer.

To solve the problem, we use essentially the same techniques in *Cane and du Penhoat* [1982] and *du Penhoat et al.* [1983]. Let $(\hat{u}, \hat{h})$ be the low-frequency incoming Rossby waves. The flow satisfies the geostrophic relation $y\hat{u} + \hat{h}_y = 0$ and is orthogonal to the Kelvin wave:

$$[(\hat{u}, \hat{h}), (\psi_0, \psi_0)] \equiv \int_{-\infty}^{+\infty} (\hat{u} + \hat{h})\psi_0 dy = 0 \qquad (1b)$$

The boundary conditions to be satisfied at $x = 0$, the longitude of the coast, are

$$u = 0 \qquad \text{for} \quad y > a \quad \text{and} \quad y < b \qquad (2)$$

i.e., at the coasts.

$$u(0_+ = u(0_-), h(0_+) = h(0_-) \qquad \text{for} \qquad b < y < a \qquad (3)$$

i.e., u and h are continuous across the gap.

At the eastern side of the coast and into the gap, the solution can be written $u^E = T^R\psi_0 + \hat{u} - \chi_y$, $h_E = T^R\psi_o + \hat{h} + y\chi(y)$, where $T^R\psi_0$ is the component of the reflected Kelvin wave. Since (u^E, h^E) satisfy the geostrophic relation, and $(\hat{u}, \hat{h})$ and the Kelvin wave do as well, substituting (u^E, h^E) in (1a) implies that $\chi(y) = 0$ for $b < y < a$. Therefore there is no short Rossby wave disturbance inside the gap.

Using the first boundary condition, (2a), we have $u = u_{Interior} + u^B = 0$ at the coast. Then we end up with a relation for the boundary layer stream function:

$$\chi(y) = \int_{-\infty}^{y} \hat{u}dy + \int_{-\infty}^{y} T^R\psi_o dy \qquad y \le b \qquad (4a)$$

$$\chi(y) = \int_{a}^{y} \hat{u}dy + \int_{a}^{y} T^R\psi_o dy + C \qquad y \ge a \qquad (4b)$$

with C a constant.

Along the coast, $x = 0$, $h = T^R\psi_o(b) + \hat{h}(b)$ at $y = b_+$, and $h = T^R\psi_o(b) + \hat{h}(b) + \chi(b)$ at $y = b_-$. (Similar formulas hold at $y = a$.) Discontinuties in h are thus possible at $y = b$ and $y = a$. Since west of the boundary u and h are in geostrophic balance, we must allow for the possibility of an infinite zonal velocity at $y = b$ and $y = a$ to balance the jump in h; that is, with δ denoting the Dirac delta function,

$$u = A\delta(y - a) + B\delta(y - b) \text{ at } y = a, b$$

We have now the complete solution at $x = 0_+$ for all y:

$$u = \hat{u} + T^R\psi_o(y) + A\delta(y-a) + B\delta(y-b), \quad h = \hat{h} + T^R\psi_o(y) \quad b \le y \le a \qquad (5a)$$

$$u = 0, \quad h = \hat{h} + T^R\psi_o(y) + y\left(\int_{-}^{y} \hat{u}dy + T^R\int_{-\infty}^{y}\psi_o\right) \quad y < b \qquad (5b)$$

$$u = 0, \quad h = \hat{h} + T^R \psi_o(y) + y\left(\int_a^y \hat{u}dy + T^R \int_a^y \psi_o dy + C\right) \quad y > a \tag{5c}$$

Continuity yields the result that (4a) is the solution at $x = 0_-$, to the west of the gap.

Using the expression for the boundary layer velocity component V^B and for the stream function χ (i.e.,equation (3b) yields

$$\int_{0+}^{+\infty} v(y = b)dx = -B = -\chi(b)$$

$$B = \int_{-\infty}^{+b} \hat{u}dy + T^R \int_{-\infty}^{b} \psi_o \tag{6}$$

The boundary current at $y = a$ is fed by the boundary current along the north-south coast. The former has transport A, while the latter has a total transport - C at $y = a$. Therefore

$$A = -C = \int_a^{\infty} (\hat{u} + T^R \psi_o)dy \tag{7}$$

To get T^R, the amplitude of the reflected Kelvin wave, we use the orthogonality and completeness properties of the eigenfunction of the shallow-water equations (cf. CS I, CS II, CS III). First, project the Kelvin wave onto the solution west of the gap (4a); i.e., use the definition (1b), noting that west of the gap the integrals extend only from $y = a$ to $y = b$. Next, use (5) and (6) to eliminate A and B. Since there is no Kelvin wave west of the gap, the projection onto (4a) is zero, and we obtain

$$T^R = -\frac{\int_b^a (\hat{u} + \hat{h})\psi_0 dy + \psi_0(a)\int_a^{\infty} \hat{u}dy + \psi_0(b)\int_{-\infty}^{b} \hat{u}dy}{2\int_b^a \psi_0^2 dy + \psi_0(a)\int_a^{\infty} \psi_0 dy + \psi_0(b)\int_{-\infty}^{b} \psi_0 dy} \tag{8}$$

The expressions for T^R, A, and B determine the complete solution. They are plotted in Figures 1a - 1c for the $n = 1, 2$, and 3 Rossby waves for different gap sizes d and different positions of the gap central latitude, $a_* = (a + b)/2$.

For the $n = 1$ Rossby mode, the amplitude of the reflected Kelvin wave is sensitive to the position of the gap. If the gap is centered on the equator ($a_* = 0$), the reflected Kelvin wave amplitude is minimum. For example, $T^R = 0.45T^{\infty}$ for $a_* = 0$, with T^{∞} the value of the reflected Kelvin wave for a full boundary, and $T^R = 0.7T^{\infty}$ if $a_* = 1$. As d becomes small, $d = a - b = \varepsilon \ll 1$, then

$$T^R \approx -\frac{\int_{-\infty}^{+\infty} \hat{u}}{\int_{-\infty}^{+\infty} \psi_0 dy} + 0(\varepsilon) = T^{\infty} + 0(\varepsilon)$$

$$A + B = O(\varepsilon)$$

All the incident mass flux is returned in the reflected Kelvin wave. As expected, when the gap is large, nothing is reflected and $T^R \approx 0$. Plots for the $n = 2$ and $n = 3$ Rossby waves show more structure, since, as n increases, waves are less equatorially trapped and have a more complex oscillating structure. The $n = 2$ mode, being antisymmetric about the equator, would generate no Kelvin wave at a full boundary. Here there is some reflection when the gap is not centered on the equator.

These results apply to the case of a basin terminated by a narrow part with a zonally infinite extent, as in Figure 2a (a zonally infinite gap). We now study the case where the gap has a finite width $L = x_2 - x_1$ (see Figure 2b). The length L is inconsequential as long as it is small compared to the zonal scale of variation of the flow,

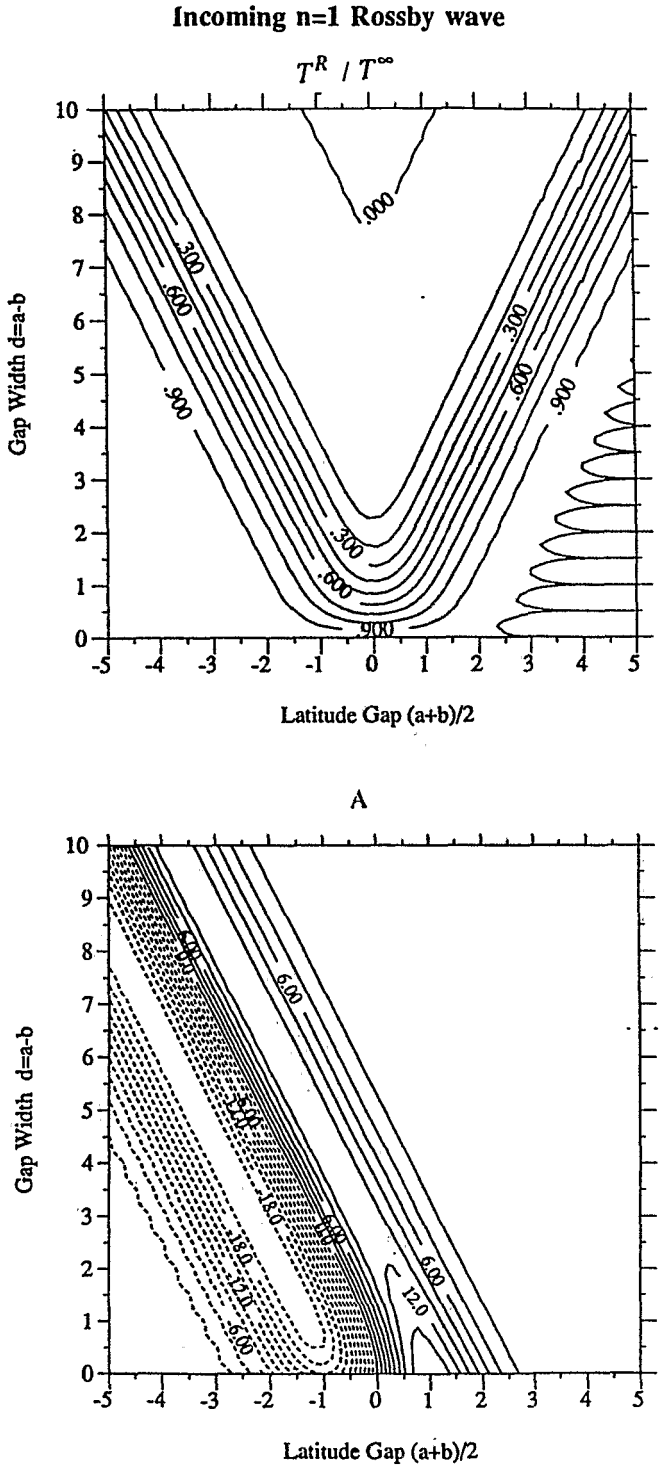

Fig.1a. Amplitude of the reflected Kelvin wave T and the boundary current transport A at $y = a$ for an incoming $n = 1$ rossby wave, for a gap of infinite zonal extent, as a function of the latitude of the gap and of its width. T has been normalized by T_{∞} (see text) for $n = 1$ has been multiplied by 100.

in which case L can be taken to be infinitesmal, as in the work by *Cane and du Penhoat* [1982]. We apply the same method as above, but now divide the domain in three regions: the downstream region west of the gap (with indices 1), the inside the gap region (indices 2), and the upstream region (indices 3). At $x = x_1$, the boundary condition $u = 0$ for $y > a$ and $y < b$, together with the geostrophic

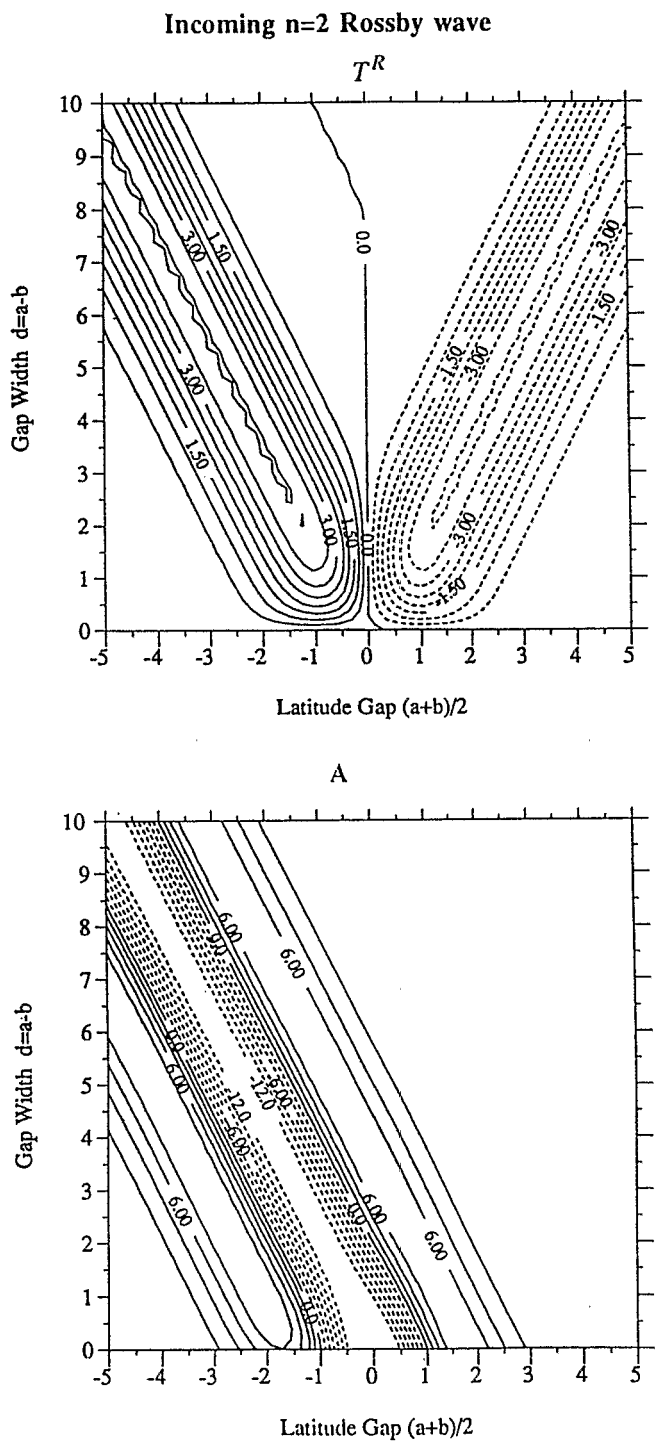

Fig.1b. Same as Figure 1a, except for $n = 2$ Rossby wave. A and T have been multiplied by 100.

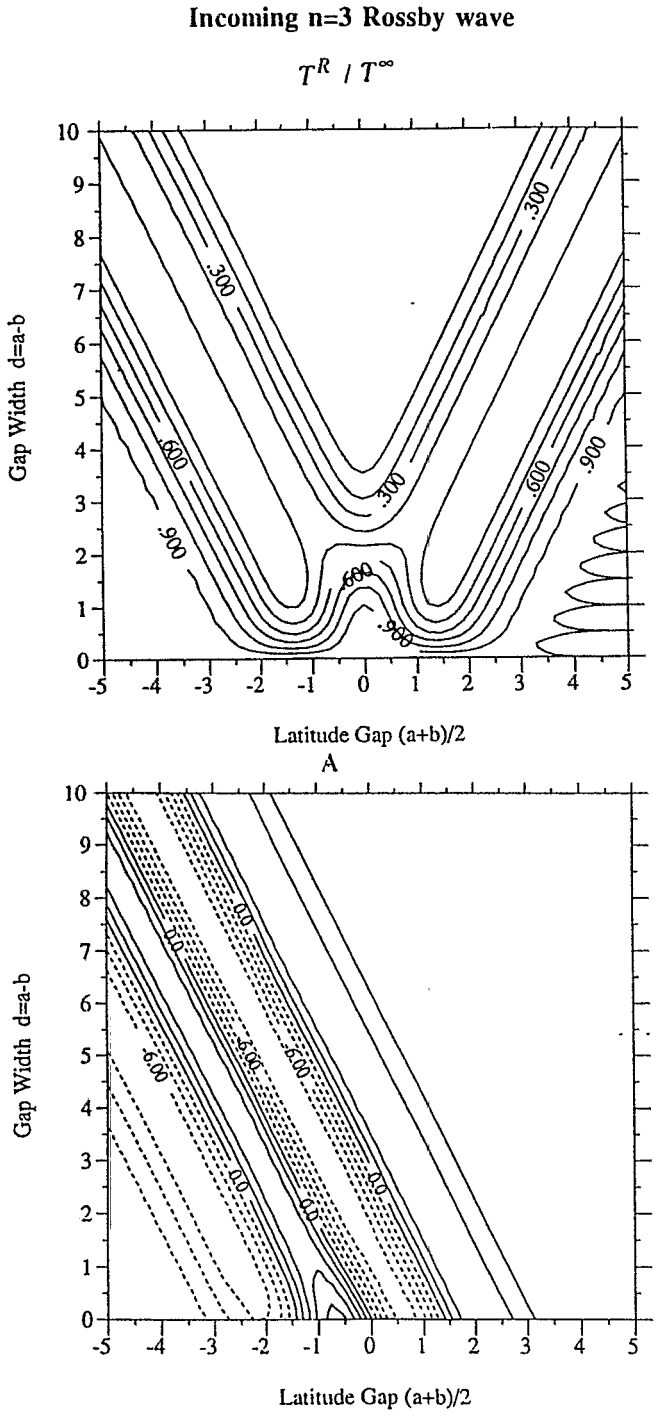

Fig.1c. Same as Figure 1a, except for $n = 3$ Rossby wave. T has been normalized by T^∞ (see text). A has been multiplied by 100.

relation (1), leads to $h = D_a$ = constant for $y > a$ and $h = D_b$ = constant for $y < b$. The total flow for the three regions is then as follows (cf. Figure 2b).

Region 1 $(u_1, h_1) + [A\delta(y-a) + B\delta(y-b), 0]$ $b \le y \le a$
$u = 0, h = D_a$ $y > a$
$u = 0, h = D_b$ $y < b$

There is no Kelvin wave in region 1.

Region 2 $(u_2, h_2) + [A\delta(y-a) + B\delta(y-b), 0] + T_2(\psi_0, \psi_0)$

Region 3 $(\hat{u}, \hat{h}) + T_3(\psi_0, \psi_0) + (-\chi_y, y\chi)$

As before, $(\hat{u}, \hat{h})$ is the Rossby wave incoming from region 3. Integrating the geostrophic relation from $y = a_+$, to $y = a_-$ and from b_- to b_+ yields

$$D_a = h_2(a) - aA + T_2\psi_0(a)$$

$$D_b = h_2(b) + bB + T_2\psi_0(b)$$

For $b \le y \le a$, u and h must be continous at the longitudes $x = x_1$ and $x = x_2$; therefore

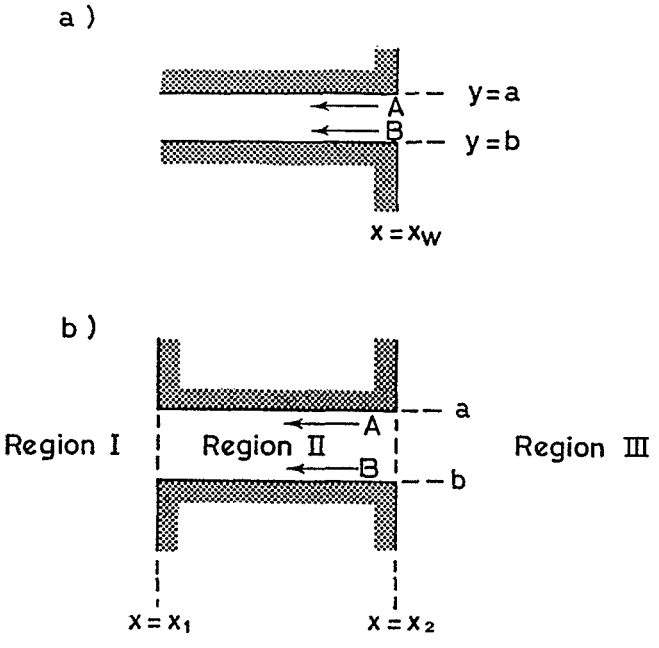

Fig.2. Schematic representation of the gap.

$$u_1 = u_2 + T_2\psi_0 + A\delta(y-a) + B\delta(y-b)$$

$$h_1 = h_2 + T_2\psi_0$$

$$u_2 + T_2\psi_0 = \hat{u} + T_3\psi_0$$

$$h_2 + T_2\psi_0 = \hat{h} + T_3\psi_0$$

As previously, A and B are determined to match the western boundary flows at $x = x_2$ in region 3, which must terminate when the walls end at $y = a$ and $y = b$:

$$A = \int_a^{\infty} \hat{u} + T_3 \int_a^{\infty} \psi_0$$

$$B = \int_{-\infty}^{b} \hat{u} + T_3 \int_{-\infty}^{b} \psi_0$$

Since there is no Kelvin wave in region 1, projecting a Kelvin wave onto the solution in region 1 yields

$$0 = \int_b^a (u_1 + h_1)\psi_0 + D_a \int_a^{\infty} \psi_0 + D_b \int_{-\infty}^{b} \psi_0$$

And therefore the expression for the reflected Kelvin wave amplitude in region 3 is

$$T_3 = -\left[\int_b^a (\hat{u} + \hat{h})\psi_0 + \psi_0(a)\int_a^{\infty} \hat{u} + \psi_0(b)\int_{-\infty}^{b} \hat{u}\right.$$

$$\left. + \hat{h}(a)\int_a^{+\infty} \psi_0 + \hat{h}(b)\int_{-\infty}^{b} \psi_0 - a\int_a^{\infty} \hat{u}\int_a^{\infty} \psi_0 + b\int_{-\infty}^{b} \hat{u}\int_{-\infty}^{b} \psi_0\right]$$

$$\times\left[2\int_b^a \psi_0^2 + 2\psi_0(a)\int_a^{\infty} \psi_0 + 2\psi_0(b)\int_{-\infty}^{b} \psi_0\right.$$

$$\left. + b\left(\int_{-\infty}^{b} \psi_0\right)^2 - a\left(\int_a^{\infty} \psi_0\right)^2\right]^{-1} \quad (9)$$

T_3 in this case is equivalent to T^R in the previous case. It differs because sea level height must be set up at the coast on the other side, in region 1. Note that T^3 agrees with *Cane and du Penhoat's* [1982] result for a two island case, one extending from $-\infty$ to b and the other from a to $+\infty$.

Figures 3a -3c show the results for this case with the $n = 1, 2, 3$ Rossby modes. In general, this geometry is a far less effective reflector than the previous case. Though in some respects it presents the same kind of pattern as in the former case, striking differences exist. For example, for a gap centered at the equator, the amplitude of the reflected Kelvin wave is still minimum compared to an off-equatorial gap, but the reflected Kelvin wave is much weaker than the former case: for the $n = 1$ incoming Rossby mode and $d = 1$, if $a_* = 1$, then $T_3 = 0.3$ instead of 0.7 and if $a_* = 0, T_3 = -0.1$ instead of 0.45.

When the gap is small ($d \to 0$), we might expect the same answer as before, i.e., that all the mass flux is reflected into the Kelvin wave. In fact, for the $n = 1$ Rossby wave, this is true only if $|a_*| > 2$. As a_* moves toward the equator, the amplitude of the reflected Kelvin wave decreases and when the pinhole is situated right on the equator, all the flow just goes through and none is reflected (Figure 4). We can analyze this case as follows: as $a, b \to a_* = \frac{1}{2}(a+b)$, $a - b = \varepsilon << 1$:

$$T_3 \approx \frac{\psi_*\int_{-\infty}^{+\infty} \hat{u} + \hat{h}_*\int_{-\infty}^{+\infty} \psi_0 - a_*[\int_{a_*}^{\infty} \psi_0 \int_{a_*}^{\infty} \hat{u} - \int_{-\infty}^{a_*} \psi_0 \int_{-\infty}^{a_*} \hat{u}]}{2\psi_*\int_{-\infty}^{+\infty} \psi_0 - a_*[\int_{-\infty}^{+\infty} \psi_0 dy(\int_{a_*}^{\infty} \hat{u} - \int_{-\infty}^{a_*} \hat{u})]} \quad (10)$$

where ψ_* stands for $\psi(a_*)$ and h_* for $h(a_*)$

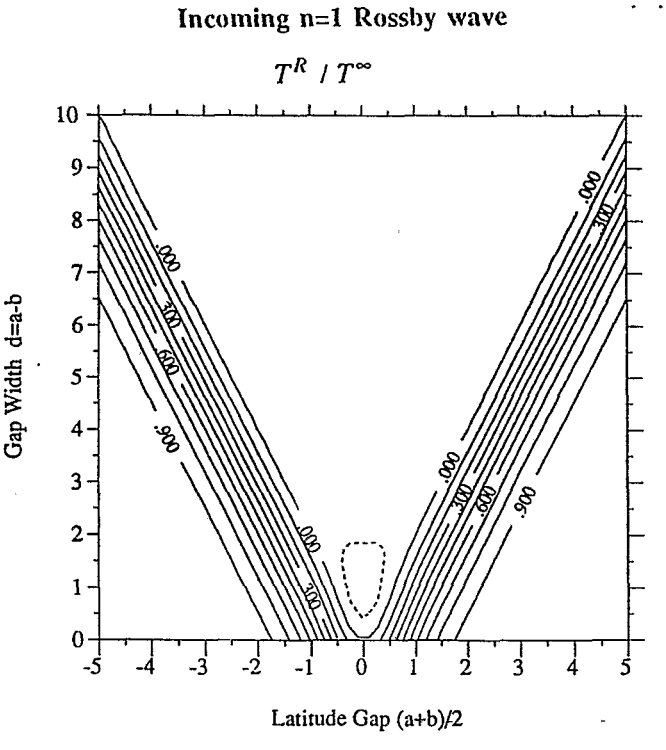

Fig.3a. Same in Fig. 1a, but for a gap of finite zonal extent. D_A, the constant height in the western side of the gap north of a, has been multiplied by 100.

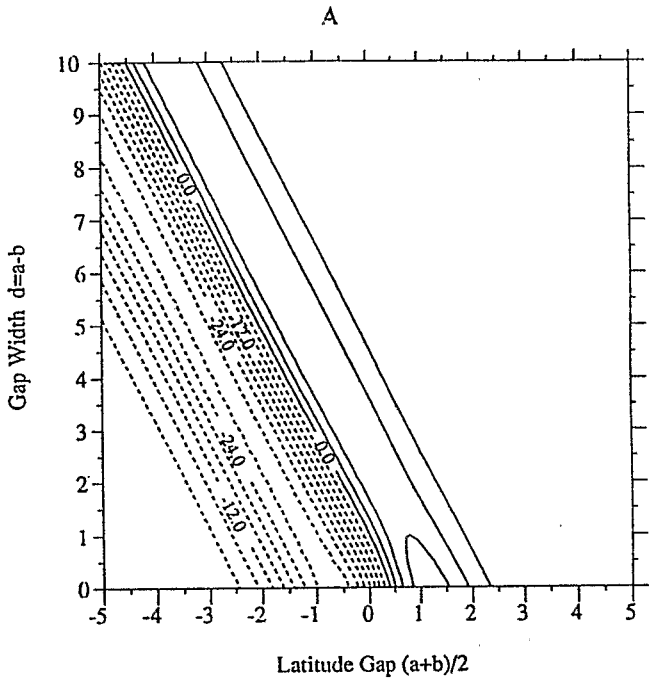

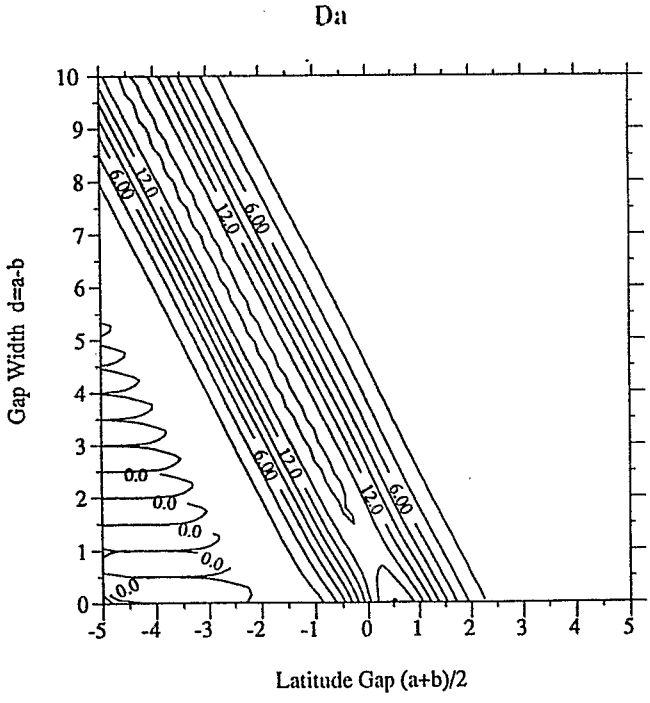

Fig. 3a. (continued)

$$A+B=\int_{-\infty}^{+\infty}\hat{u}dy+T_3\int_{-\infty}^{+\infty}\psi_0 dy \qquad (11)$$

$$D_a=\hat{h}_*+T_3\left(\psi_*+\int_{-\infty}^{+\infty}\psi_0 dy-\int_a^{\infty}\psi_0\right)+a_*\left(\int_{-\infty}^{+\infty}\hat{u}dy-\int_a^{\infty}\hat{u}dy\right) \qquad (12)$$

As $a_* \to 0$

$$T_3 \approx \frac{\psi_*\int_{-\infty}^{+\infty}\hat{u}+\hat{h}_*\int_{-\infty}^{+\infty}\psi_0 dy}{2\psi_*\int_{-\infty}^{+\infty}\psi_0 dy}$$

Therefore the solution is determined by the values of ψ_o and $\hat{h}$ at the equator and the integrated incident mass flux. For the $n = 1$ Rossby wave,

$$\int_{-\infty}^{+\infty}\hat{u}dy=-\hat{h}(0)\int_{-\infty}^{+\infty}\psi_0'\psi_0(0)$$

and we have the unexpected result that all the flow goes through the delta function gap and nothing is returned in the Kelvin wave. All the incoming mass flux is in the boundary currents $A + B$, and the height set up on the other side of the gap is equal to $\hat{h}(0)$. This case differs from the previous one because the mass flux must escape through to set up a constant sea level on the other side.

We can compute the amplitude of the Kelvin wave reflected at $x = x_1$, by noting that there is no Kelvin wave in region 1. Then,

$$T_2\int_b^a\psi_0^2dy=\int_b^a(\hat{u}+\hat{h})\psi_0 dy+T_3\{\int_b^a\psi_0^2dy$$

$$+\psi_0(a)\int_a^{\infty}\psi_0 dy+\psi_0(b)\int_{-\infty}^{b}\psi_0 dy\}$$

$$+\{\psi_0(a)\int_a^{\infty}\hat{u}dy+\psi_0(b)\int_{-\infty}^{b}\hat{u}dy\}$$

As the gap width becomes small, i.e., $d = a - b = \varepsilon << 1$, asymptotic expansion yields

$$\varepsilon T_2\psi_*=T_3\int_{-\infty}^{+\infty}\psi_0 dy+\int_{-\infty}^{+\infty}\hat{u}dy+O(\varepsilon)$$

or, using (10)

$$\varepsilon T_2\psi_*=A+B$$

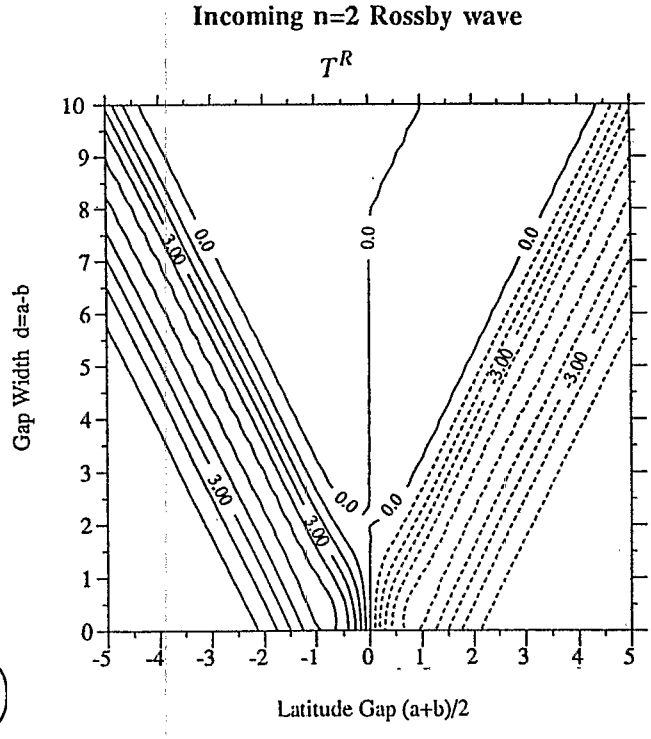

Fig.3b. Same as Figure 1b, but for a gap of finite zonal extent.

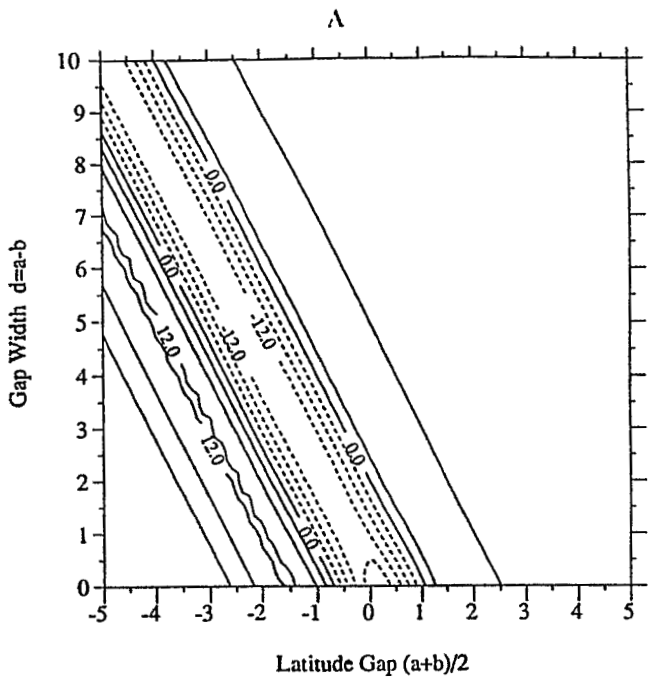

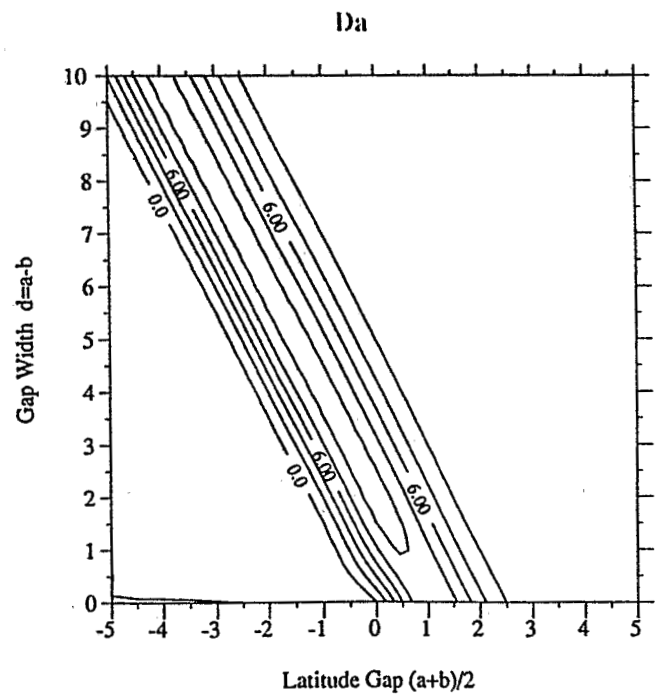

Fig. 3b. (continued)

Therefore if the boundary currents $A+B$ are not small, the amplitude of the reflected Kelvin wave at the end of the gap must be large in order to balance the incoming flux and $T_2 \sim O(\varepsilon^{-1})$.

In case of a gap at $a_* = 0$:

$$\varepsilon T_2 \psi_* = -\frac{1}{2}\int_{-\infty}^{+\infty} \hat{u}dy - \frac{\hat{h}}{2\psi_*}\int_{-\infty}^{+\infty} \psi_0 dy + \int_{-\infty}^{+\infty} \hat{u}dy$$

$$D_a = D_b = \frac{1}{2}\hat{h}_* - \frac{\psi_*}{2}\frac{\int_{-\infty}^{+\infty} \hat{u}dy}{\int_{-\infty}^{+\infty} \psi_0 dy}$$

In Figure 4, the amplitude of the reflected Kelvin wave is plotted for different incoming Rossby waves as a function of latitude a_* with a zero width gap. For n odd, the gap is not felt if it is situated outside the turning latitude [$Y_T \sim (2n+1)^{1/2}$]: all the incoming mass flux is then returned in the reflected Kelvin wave and $A+B \sim O(\varepsilon)$. For n even ($\hat{u}$ and $\hat{h}$ are antisymmetic), with a gap outside the turning latitudes, the solution is the same as for the full boundary: there is no reflected Kelvin wave, since with this symmetry there is no net mass flux into the western boundary.

3. Incident Delta Function Flow on a Gap

In this section, we solve the problem for cases where all the incident mass is poleward (or equatorward) of the gap. Specifically, we assume an incoming velocity of delta function form impinging on the boundary at a latitude s; i.e., $\hat{u} = -\delta(y-s)$. Since $\hat{u}$, $\hat{h}$ must satisfy the geostrophic relation, $\hat{h} = -[h_s - sH(y-s)]$, where $H(y-s)$ is the Heaviside step function:

$$H(y-s) = 1 \qquad y > s$$

$$H(y-s) = 0 \qquad y > s$$

The condition of no Kelvin wave requires that

$$h_s = -\left(\int_{-\infty}^{+\infty} \psi_0 dy\right)^{-1} \int_s^{\infty} (s-y)\psi_0 dy$$

The solution may be thought as a Green's function and different forms of the incoming flow can be found from an integral equation using this Green's function solution. As before, we consider the two different geometries of Figure 2.

3.1. *Western Boundary With a Zonally Infinite Gap (Figure 2a)*

The same methods apply and we just plug the form of $\hat{u}, \hat{h}$ in the solutions of section 2. We separate the solution into three cases: (1) The latitude s of the incoming flow is poleward of the latitude of the gap: $s > a > 0$: The amplitude of the reflected Kelvin wave is

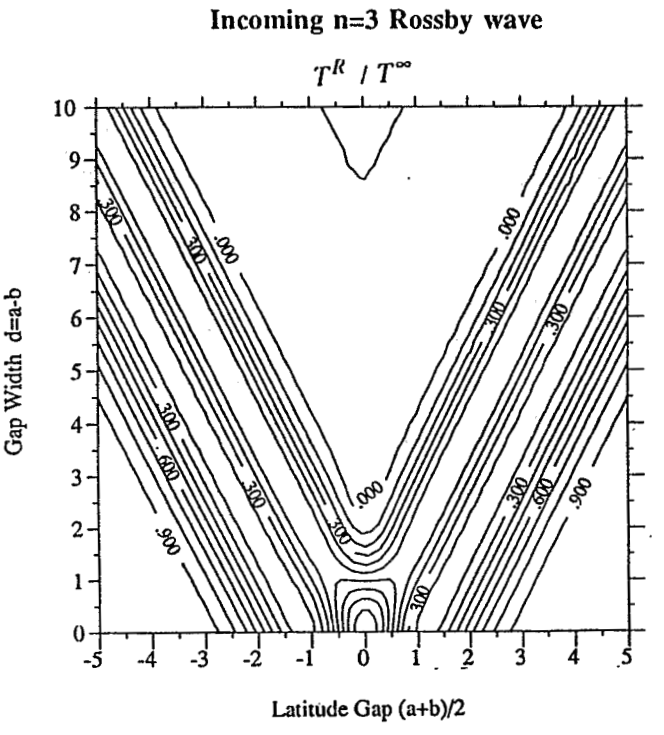

Fig.3c. Same as Figure 1c, but for a gap of finite zonal extent.

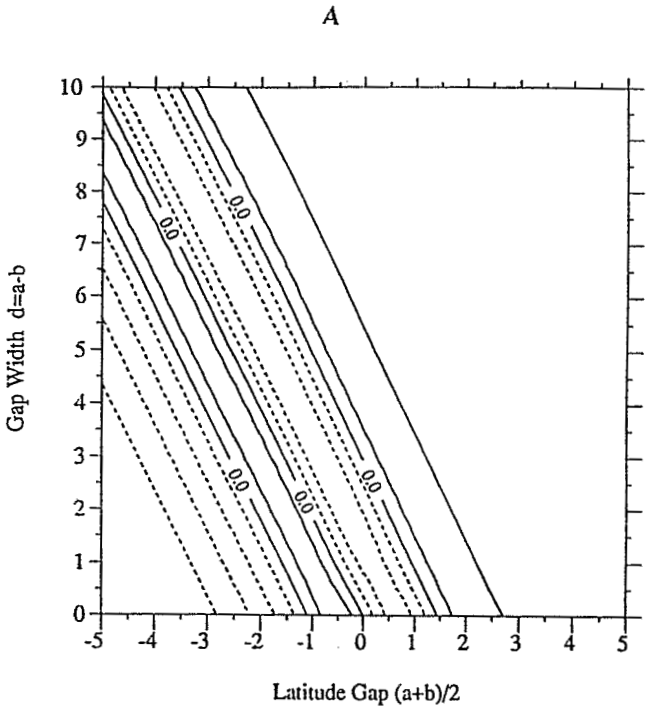

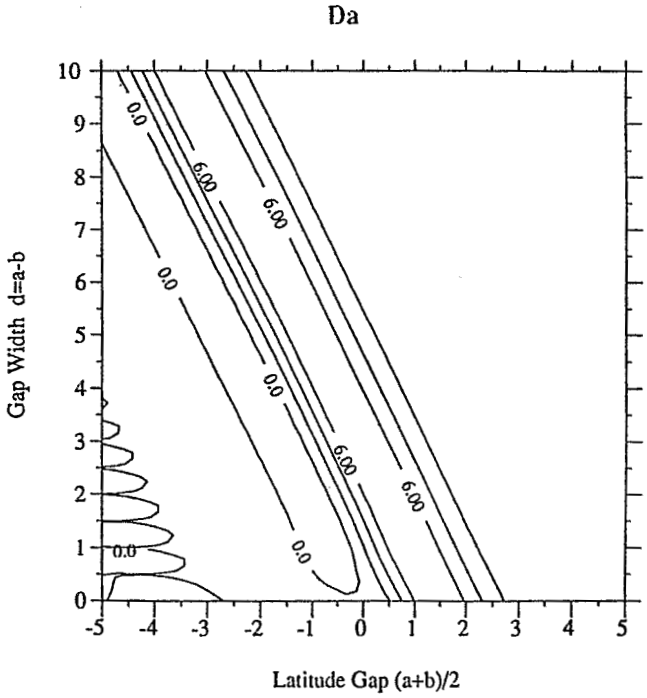

Fig. 3c. (continued)

$$T = \frac{1}{P\int_{-\infty}^{+\infty}\psi_0 dy}\left[s\int_b^a \psi_0 dy \int_s^{\infty}\psi_0 dy - \psi_0(s)\int_b^a \psi_0 dy + \psi_0(a)\int_{-\infty}^{+\infty}\psi_0 dy\right] \quad (13)$$

with

$$P = 2\int_b^a \psi_0^2 dy + \psi_0(a)\int_a^{\infty}\psi_0 dy + \psi_0(b)\int_{-\infty}^{b}\psi_0 dy \quad (14)$$

$$A = -1 + T\int_a^{\infty}\psi_0; \quad B = T\int_{-\infty}^{b}\psi_0 dy \quad (15)$$

(2) The latitude of the incident flow is within the gap: $b < s < a$. A and B are again given by (14) but

$$T = \frac{1}{P\int_{-\infty}^{+\infty}\psi_0 dy}\left[\psi_0(s)\left(\int_{-\infty}^{+\infty}\psi_0 dy - \int_b^a \psi_0 dy\right) + s\left(\int_b^a \psi_0 dy\int_s^{\infty}\psi_0 dy - \int_s^a \psi_0 dy\int_{-\infty}^{+\infty}\psi_0 dy\right)\right] \quad (16)$$

(3) For $s < b < a$, the solution is

$$T = \frac{1}{P\int_{-\infty}^{+\infty}\psi_0 dy}\left[s\int_b^a \psi_0 dy\left(\int_s^{\infty}\psi_0 dy - \int_{-\infty}^{+\infty}\psi_0 dy\right) - \psi_0(s)\int_b^a \psi_0 dy + \psi_0(b)\int_{-\infty}^{+\infty}\psi_0 dy\right] \quad (17)$$

$$A = T\int_a^{\infty}\psi_0 dy; \quad B = -1 + T\int_{-\infty}^{b}\psi_0 dy \quad (18)$$

Figure 5 shows the solution for $d = 1$ as a function of the latitude of the gap and the latitude of the incoming flow. In Figure 5, the amplitude T_* has been normalized by the value of T when the boundary is a full boundary (i.e., when $d = 0$). As $a - b \to 0, T \to T_\infty = [\int_{-\infty}^{+\infty}\psi_0 dy]^{-1} + O(\varepsilon)$. If the latitude of the flow and the latitude of the gap are on opposite sides of the equator, most of the incoming mass flux is reflected in the Kelvin wave. For example, for $d = 1$, $T \sim 0.9$, if $a_* < -1$ and $s > 0$: the flow behaves as if it does not feel the gap.

If the latitude of the forcing and the latitude of the gap are on the same side of the equator, the amplitude of the reflected Kelvin wave decreases, and the flux of the boundary currents increases. A and B are in opposite directions and most of the mass flux goes into the boundary current closer to the incoming flow and has the same direction.

If the latitude of the incoming flow is between the latitudes of the gap, the amplitude of the reflected Kelvin wave is reduced compared to cases where it hits the boundary outside of the gap, but the amplitude is not negligible, with a maximum occurring at the equator.

In all cases, the reflected Kelvin wave is negligible only when s and a are far from the equator, depending also on the position of s and a_* relative to the equator.

3.2. *Finite Longitudinal Width Gap (Figure 2b)*

As noted in the previous section, the long wave approximation makes the finite longitudinal width gap equivalent to an infinitesimally thin gap. The solution is obtained by using results of section 2 (see equation 8 and following): (1) $s > a > o$:

$$T = \frac{1}{P}\left[\psi_0(a) - \psi_0(s) + s\int_s^{\infty}\psi_0 dy - a\int_a^{\infty}\psi_0 dy\right] \quad (19)$$

with

$$P = 2\int_b^a \psi_0^2 + 2\psi_0(a)\int_a^{\infty}\psi_0 + 2\psi_0(b)\int_{-\infty}^{b}\psi_0 + b\left(\int_{-\infty}^{+\infty}\psi_0\right)^2 - a\left(\int_a^{\infty}\psi_0\right)^2 \quad (20)$$

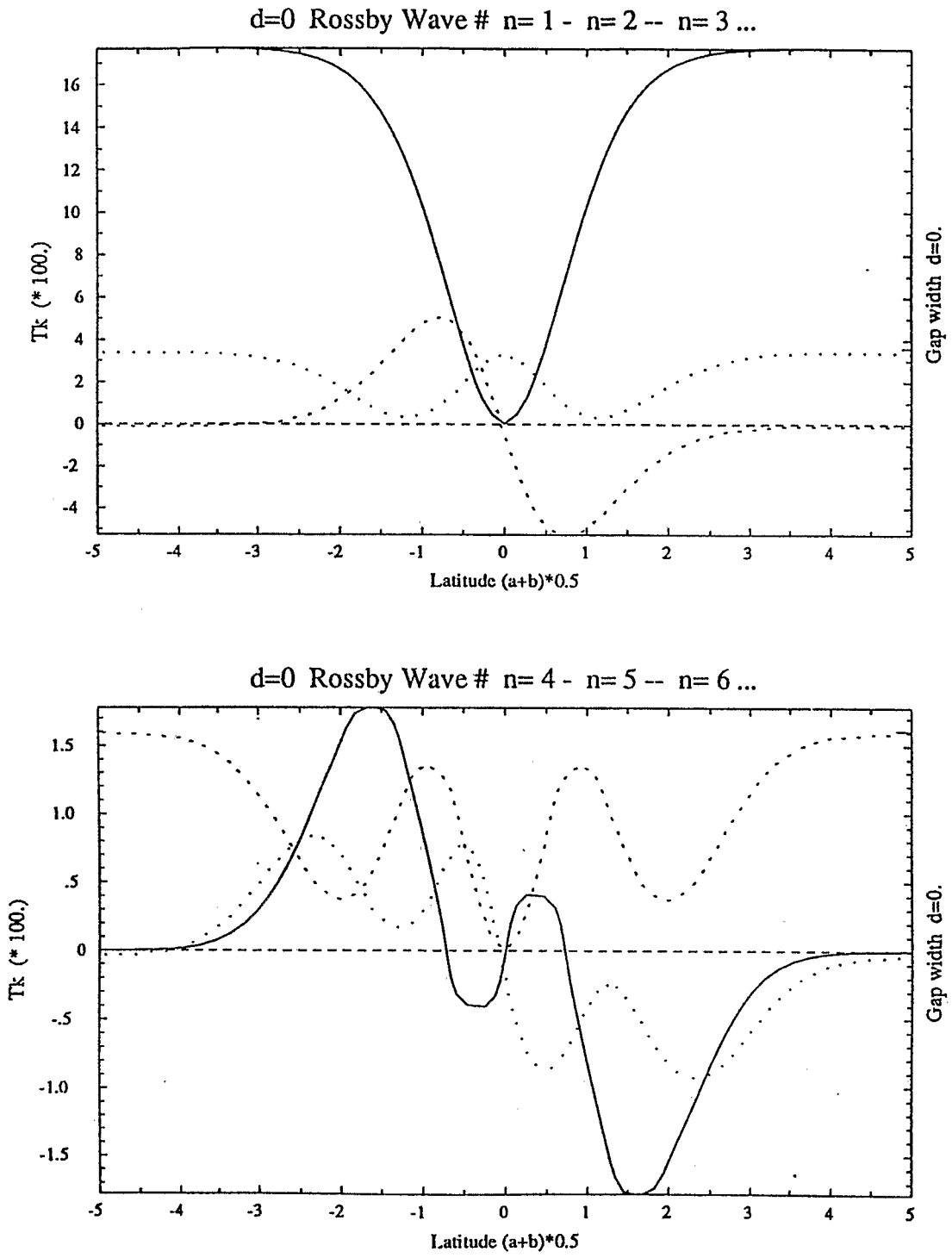

Fig.4. Amplitude of the reflected Kelvin wave (*100) for $n = 1$ - 6 Rossby waves for the case of a pinhole-sized gap ($d = 0$) as a function of the gap latitude.

$$A = -1 + T\int_a^\infty \psi_0 dy; \quad B = T\int_{-\infty}^b \psi_0 dy \tag{21}$$

$$D_A = h_s + T\psi_0(a) - aA \tag{22}$$

$$D_B = h_s + T\psi_0(b) + bB \tag{23}$$

(2) $b < s < a$: There is no reflected Kelvin wave: $T = 0$, . $A = B = 0$, and the sea level on the western side of the gap is simply $D_A = \hat{h}(a) = h_s - s$ and $D_B = \hat{h}(b) = h_s$. The incoming flow *passes* through the gap unperturbed.

(3) $s < b$:

$$T = \frac{1}{P}\left[\psi_0(b) - \psi_0(s) + s\left(\int_s^\infty \psi_0 dy - \int_b^a \psi_0 dy\right) - a\int_a^\infty \psi_0 dy\right] \tag{24}$$

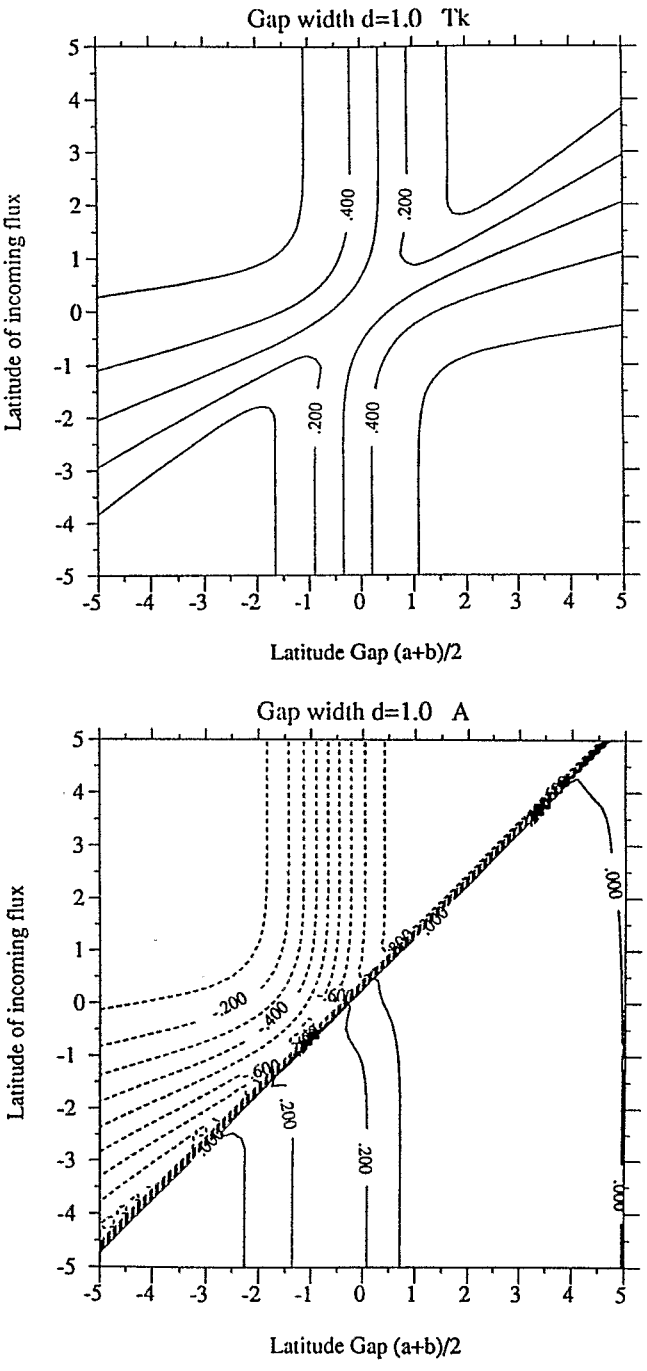

Fig.5. Amplitude of the reflected Kelvin wave T_K and boundary current transport A as a function of the latitude of the incoming δ mass flux and the latitude of the gap. For a gap of width $d = 1$ and infinite zonal extent.

$$A = T\int_a^\infty \psi dy; \quad B = -1 + T\int_{-\infty}^b \psi_0 dy \tag{25}$$

$$D_A = T\psi_0(a) - aA + h_s - s \tag{26}$$

$$D_B = T\psi_0(b) + bB + h_s - s \tag{27}$$

The solution is plotted in Figures 6. The behavior is identical to the previous case, if the latitude of the forcing flow and the latitude of the gap are on opposite sides of the equator: T_* $(= T/T_\infty) \approx 0.9$, A and B are small, as are D_A and D_B. As a_* and s get closer, T_* decreases ($T_* \to 0$), $A \to 1$ and $B \to 0$, if s is north of the equator; if s is south, then $B \to 1$ and $A \to 0$).

This case differs from the former case if the latitude s of the incoming flow is between a and b. There is no reflected Kelvin wave, $A = B = 0$, and there is a height deviation on the downstream side of the gap. If S and a_* are both north of the equator, D_A is large and D_B is small (conversely, D_B is large and D_A small, if s and a_* are both south of equator.)

4. THE WESTERN PACIFIC CASE

It has been suggested that reflections of Rossby waves on the western boundary of the Pacific Ocean are intrinsic to the development of ENSO events. We will try to get some insight from our theory into reflections at the Indonesian archipelago and the associated flowthrough between the Pacific and Indian Oceans. Pertinent observations were briefly reviewed in section 1.

We wish to calculate the flow through the Indonesian archipelago from the Pacific to the Indian Ocean. We know from consideration of mass conservations that the mass flux through the Indonesian seas is just the difference between the incident flow (Rossby waves) and the reflected Kelvin wave flow. The partition between transmitted and reflected mass flux is determined by the way the pressure gradient adjusts to the geometry; i.e., to the pattern of the height field h. The method we developed in previous sections may be used to find h and the flowthrough.

To do so, we first must simplify the very complex geometry of this region. Actually, the assumptions made in our theory mean that this can be done without changing the results: the assumptions are certainly questionable, but once they are made, certain topological invariances are obtained. Then the flow through the complex region is the same as that through an equivalent simple geometry. We will first develop some simplifying rules and apply them to the Indonesian case.

Cane and Gent [1984] presented a theory for calculating the effect of solid sloping western boundaries on low-frequency wave reflections. The slope of the coast, γ, affects the answer, but only through the combination $\gamma\omega$, with ω being the (nondimensional) frequency. As ω goes to zero, the effect disappears. *McCalpin* [1987] applied their theory to a more realistic representation of the western Pacific boundary and found no effect on the gravest meridional and baroclinic modes. (Higher modes were affected for frequencies above the semiannual). Throughout our calculations, we have made the assumption that the frequency is low enough so that phase differences with longitude may be ignored. Thus the sloping coast may be replaced by a zig-zagging coastline in the manner so familar in numerical models, and finally by a straight coast, (namely, Figure 7a). Only the gap matters.

Similarly, while the latitude of the gap is important, the longitude is not. A gap with its northern side at a longitude and its southern side at another longitude has the same effect as when both sides of the gaps are at the same longitude: the three configurations of Figure 7b give the same reflected wave amplitude at the east and the same circulation at the west.

We now consider a bay open to the west, as in Figure 7c. At the interior north-south shoreline, at $x = x_2$, $u = 0$. In this unforced inviscid steady problem, it follows that $u = 0$ everywhere inside the bay at $x = x_3$. Hence the bay has no effect: it is as if it were filled in, part of a solid block, as in Figure 7d.

In the same vein, there is no effect from a small island directly west of a larger one (larger in latitudinal reach, so that the small one is within its "shadow"); namely, Figure 7e.

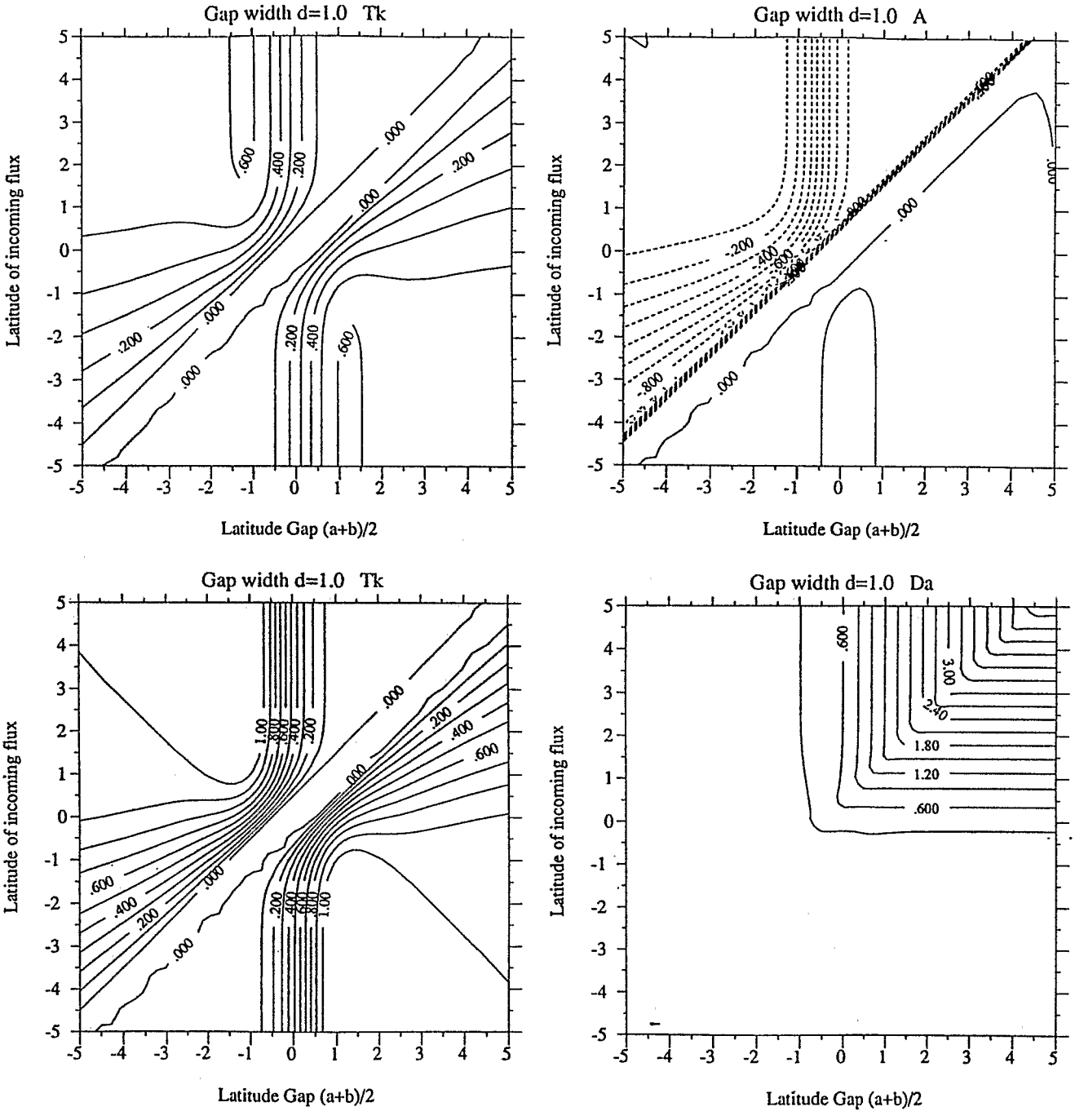

Fig.6. Same in Fig. 5, but for a gap of finite zonal extent. D_A is the constant height in the western side of the gap north of a.

If the small island is to the east, as in Figure 7f, there is again no difference from the solid block of Figure 7d, west of x_3 or east of x_1, though the circulation between x_1 and x_2 is influenced by the small island.

We finally end up with a simplified geometry, shown in Figure 8b, roughly deduced from the 400-m isobath in Figure 8a. We separate the basin geometry into segments between longitudes x_j and x_{j+1}, with $j = 1, 9$. In Figure 8b, a represents the south latitude of the land masses of Philippines, Borneo, and Asia, while b stands for the north latitide of New Guinea, Halmahera and Celebes Islands, assuming that there is no significant flow through the Molucca strait (between latitude b and latitude c). The connection to the Indian Ocean is through the Strait of Macassar (between latitude b and latitude a in Figure 8b). The latitude of the Indonesian Islands (Bali, Lombock, Timor, etc.) are between latitudes d and g or e and g. We also assume that there is no flow through the Arafura Strait. Thus in the schematized geometry of Figure 8b, segment 9 is a closed segment.

As noted previously, results for segments 5 and 6 are the same as if the longitude x_6 and x_5 were the same, and those cases have been studied in previous sections.

The segment 9 is closed by a full boundary, and we have $u_9 = 0$ and $h_9 = H = constant$. (This case is equivalent to the case e in Figure 7). Using the continuity conditions at longitude x_8, the

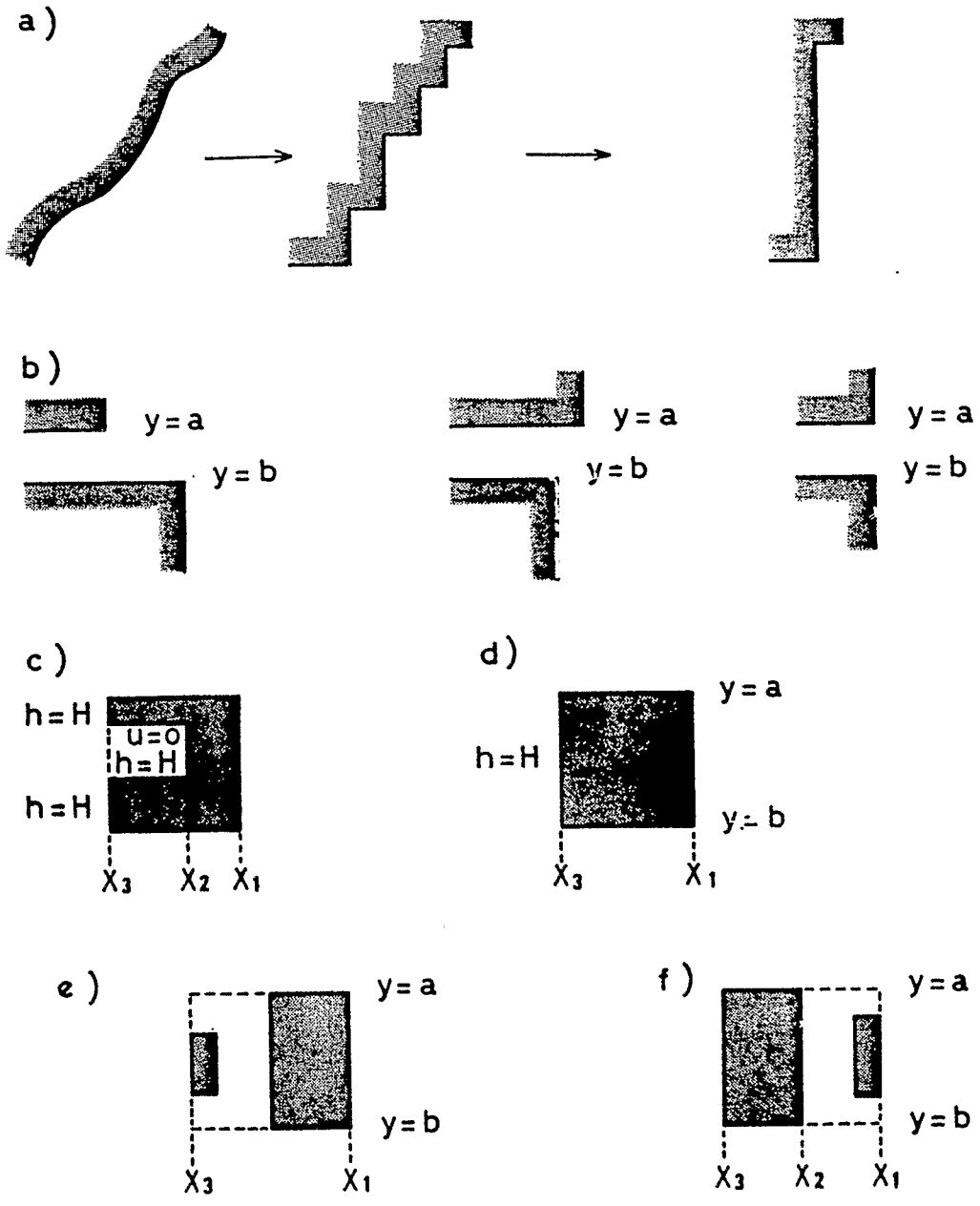

Fig.7. Some examples of equivalent representation of comples geometry (see text).

boundary longitude between segments 8 and 9, and working back to the longitude x_8, we find that there is no buondary current along the east-west coast at latitude e, and

$$T_7\psi_o + h_7 = H \tag{28}$$

$$T_7\psi_o + u_7 = 0$$

Hence at longitude x_4 (= x_7), intergrating the geostrophic relation at $y = b$ and $y = c$, we end up with

$$bB + h_4(b) + T_4\psi_o(b) - H = 0 \tag{29}$$

$$-(h_7(c) + T_7\psi_o(c)) + H = 0 \tag{30}$$

Thus we now have at the 3 - 4 boundary:

$$T_3\psi_o + u_3 = T_6\psi_o + \hat{u} + A\delta(y-a) + B\delta(y-b) \tag{31}$$

$$T_3\psi_o + h_3 = T_6\psi_o + \hat{h}$$

for $y > b$, and

$$T_3\psi_o + u_3 = 0 \tag{32}$$

$$T_3\psi_o + h_3 = H = bB + T_6\psi_o(b) + \hat{h}(b)$$

for $y < b$. It follows that at longitude x_3

$$u_2 + T_2\psi_o = u_3 + T_3\psi_o \tag{33}$$

$$h_2 + T_2\psi_o = h_3 + T_3\psi_o$$

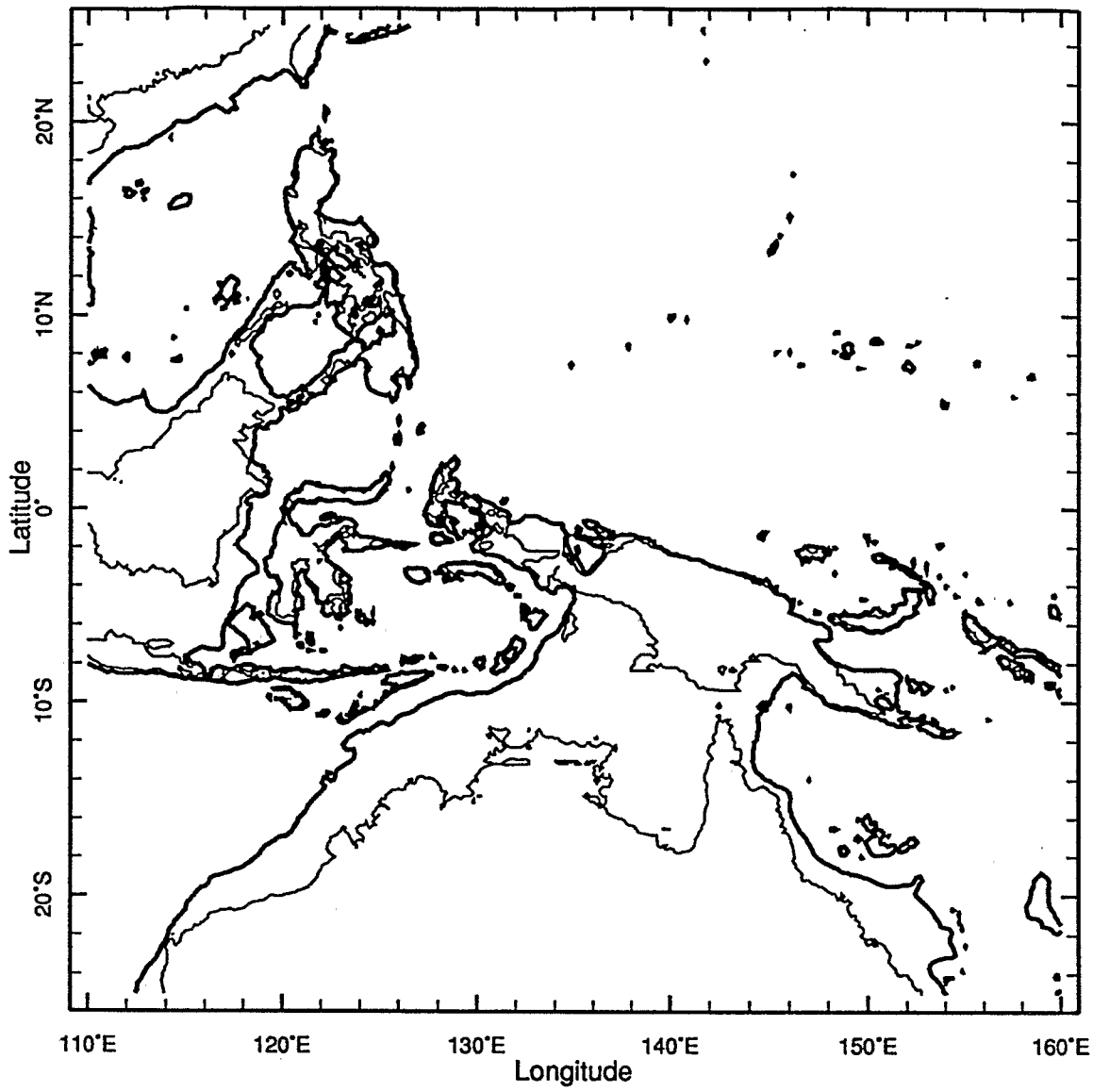

Fig. 8. (a) Map of the Pacific western boundary and the Indonesian seas.

for $y > c$, and

$$u_2 + T_2\psi_o = 0 \tag{34}$$

$$h_2 + T_2\psi_o = H_2 = h_3(e) + T_3\psi_o(e)$$

for $y < e$.

The last equality follows, since there is no boundary current along the east-west coast at latitude e.

Proceeding further west to longitude x_2:

$$T_1\psi_o + u_1 = T_2\psi_o + u_2 + D\delta(y-d) = T_3\psi_o + u_3 + D\delta(y-d) \tag{35}$$

$$T_1\psi_o + h_1 = T_3\psi_o + h_3$$

with D the boundary current transport along the east-west coast at latitude d.

At the western boundary within segment 1, the boundary condition that gives the correct long wave reflections (CS II) can be written

$$T_1\int_d^a \psi_o dy + \int_d^a u_1 dy = 0 \tag{36}$$

Using (30), (31), (34) and (35) leads to

$$T_6\int_b^a \psi_o dy + \int_b^a \hat{u} dy + A + B + D = 0 \tag{37}$$

Furthermore, we have a relation between the boundary current transports G and D *Cane and du Penhoat* [1982]:

$$G + D = \int_g^d (u_2 + T_2\psi_o)$$

In view of (33) we conclude

$$G = -D \tag{38}$$

Returning to (36), and using (37) and the relations for A and B like (5) and (6), yields

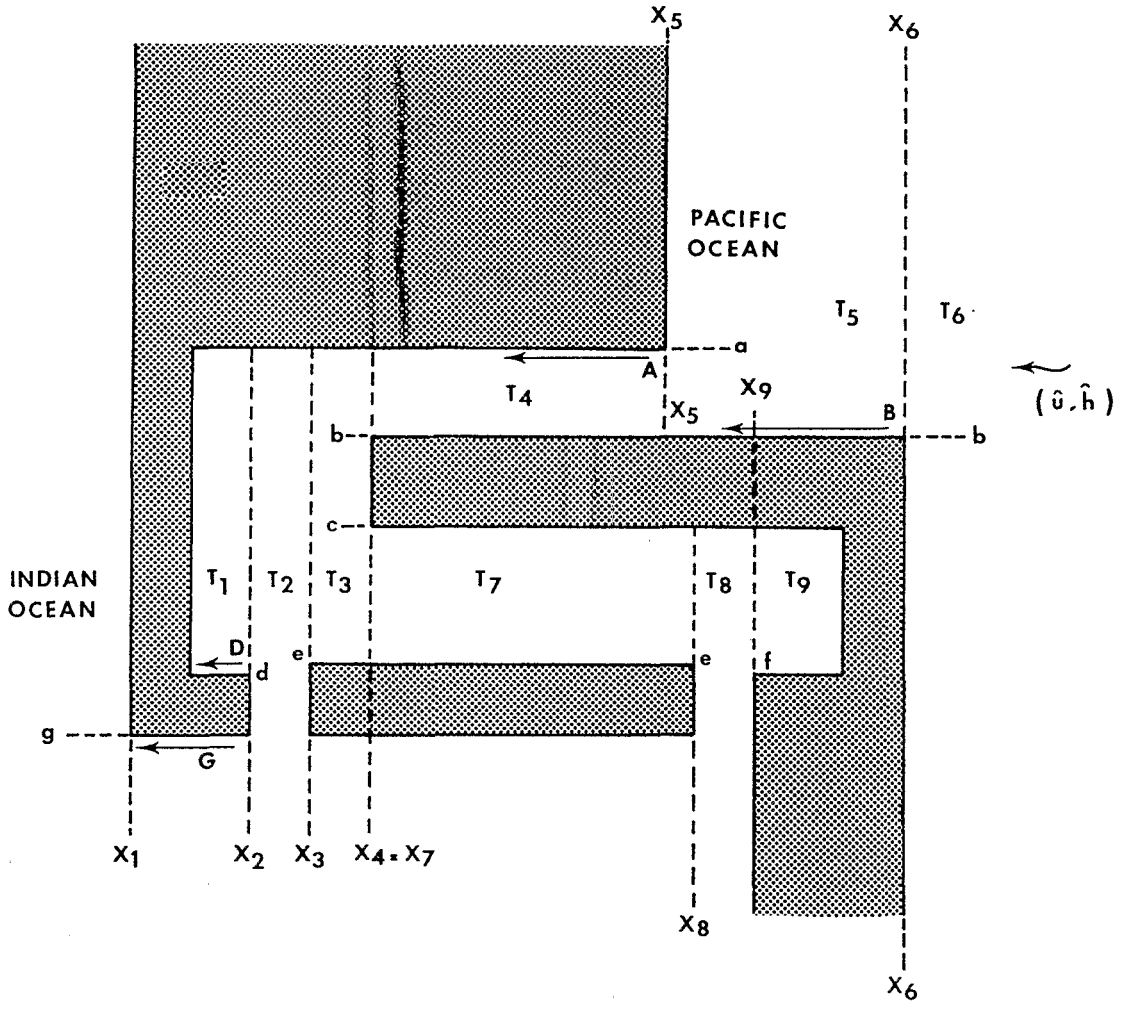

Fig. 8. (b) Schematic representation of map in Figure 8a.

$$G = T_6 + \int_{-\infty}^{+\infty} \psi_o \, dy + \int_{-\infty}^{+\infty} \hat{u} dy \tag{39}$$

i.e., the flow through G is the total incident mass flux $\hat{u}$ less the reflected Kelvin wave flux. That is, mass is conserved.

Another condition is needed to find the two unknown G and T_6 in (38). This is obtained from the relations for h, which constrains the possible pressure gradient to drive the flowthrough. Unlike (37), this will depend on the latitudinal distribution of the flow. Offshore of the boundary current G, we know from (31), (33) and (34) that the height deviation $h = H$. We assumed that there was no flow through the Arafura Strait into the Arafura Sea, so the amplitude G is then determined at the outflow point on the Indian Ocean side. So far, we have established that south of g, $u = 0$, and $h = H$, and north of g, $u = 0, h = H - gG$, using (1).

The condition that there be no Kelvin wave west of g implies

$$G\psi_o(g) + H \int_{-\infty}^{+\infty} \psi_o dy - gG \int_g^{\infty} \psi_o dy = 0 \tag{40}$$

Then we find, using (31), (38) and (39)

$$T_6 = -\left[\frac{\hat{h}(b) + b\int_{-\infty}^{b} \hat{u} dy + \left(\int_{-\infty}^{+\infty} \hat{u} dy\right)\left(\psi_o(g) - g\int_g^{\infty} \psi_o dy\right)\left(\int_{-\infty}^{+\infty} \psi_o dy\right)^{-1}}{\times\left[\psi_o(g) - g\int_g^{\infty} \psi_o dy + \psi_o(b) + b\int_{-\infty}^{b} \psi_0 dy\right]^{-1}}\right] \tag{41}$$

This result can easily be generalized to the case when an incoming Kelvin wave of amplitude K also exists on the Indian Ocean side: just add K to the right-hand side of (39). The flow south of g will also change owing to the incoming Kelvin wave flow in these parts of the basin.

The relation (40) simply indicates that the resulting amplitude of the reflected Kelvin wave in the Pacific Ocean part is independent of a, and depends only on the latitude of the Indian and Pacific Ocean entrance latitudes, i.e., g and b. This is consistent with conservation of mass and with our simplifying rules. However, the presence of a coastline at $y = a$ induces a boundary current A along the coast.

For our crude schematization of the western Pacific, we choose $b = 3°$ N (representing the Halmahera and Morotai islands) and $g = 8°5'$ S (standing for the latitude of the Lombok and Timor Straits). Figure 9 gives the computed amplitude of the reflected Kelvin wave in the Pacific Ocean for different incoming Rossby waves. Results are shown for the first three baroclinic modes. For

Vertical mode #	1			2			3		
Radius of deformation	357 km			279 km			223 km		
Mode	1	2	3	1	2	3	1	2	3
T^k	0.15	-0.016	0.026	0.16	-0.011	0.027	0.17	-0.007	0.029
$\frac{T^k}{T^=}$	0.85	-	0.74	0.91	-	0.76	0.95	-	0.79

Fig.9. Amplitude of the reflected Kelvin wave in the schematic western boundary of Figure 8b. Values are given for different vertical modes and different incoming Rossby waves.

symmetric modes ($n = 1$ and $n = 3$ in Figure 9), the amplitude of the reflected Kelvin wave increases with increasing baroclinic mode number (as the meridional scale decreases). For $n = 1$ incoming Rossby modes, the amplitude of the reflected Kelvin wave is over 85% of the amplitude of the reflected Kelvin wave for a full boundary. It is weaker for the $n = 3$ incoming Rossby wave (74% for the first baroclinic mode), as for such mode the meridional structure is less equatorially trapped. For antisymmetric (n even) Rossby modes, the presence of a gap allows a reflected Kelvin wave to exist, whereas a full boundary would not. As the baroclinic mode number increases, the amplitude of the reflected Kelvin wave decreases as the boundary tends to be more like a full boundary. Therefore as far as this theory is concerned, the western Pacific boundary acts as a substantial reflector.

5. Conclusion

In this note, we have calculated the effect of gaps on reflections at a low-latitude western boundary. The calculations are carried out within the framework of the low-frequency limit of the linear shallow-water equations and are thus highly idealized. The analytic techniques are an extension of those used by *Cane and du Penhoat* [1982] to study the effect of low-latitude islands.

The results, which we found rather surprising in some respects, may be summarized as follows. The amplitude of the reflected equatorial Kelvin wave is sensitive to the location of the gap and the structure of the incoming flow. In addition, the results can be quite different, depending on whether the zonal extent of the gap is assumed to be infinite or finite. More precisely, the latter means that the extent of the gap is short compared with the zonal wavelength of the relevant free waves. A coastline with a finite zonal length gap is a less efficient wave reflector than an infinite zonal length gap. The difference is nonnegligible if the location of the gap is close enough to the equator (i.e., within two radii of deformation). For a $n = 1$ Rossby wave, as the gap width gets smaller, the reflected Kelvin wave amplitude gets surprisingly small in the case of a finite zonal length gap. If the gap width goes to zero, there is no reflected Kelvin wave; all the incoming mass flux is in the boundary currents and is used to set up the sea level height on the other side of the gap. More generally, the size of this effect varies with the latitudinal structure of the incoming flow, because this influences the height of the sea level setup on the west coasts of the land masses bounding the gap. In contrast, when the gap is zonally infinite, there is no coast west of the gap and all the mass flux is reflected back in the Kelvin wave, as expected.

We also solved the problem for the case where the incoming velocity is taken as a delta function and the solution may be thought as a Green's function for a more complicated flow. The solution depends essentially on the latitudes of the incoming flow and of the gap relative to the equator. With a gap and an incoming flow on opposite sides of the equator, the flow behaves as if it does not feel the gap and most of the incoming mass flux is reflected in the Kelvin wave. With an infinite zonal gap, even if the incoming velocity is within the gap, there is some reflected Kelvin wave. With a finite zonal length gap, there is no reflected Kelvin wave and the flow behaves as if it does not feel the gap: there are no boundary currents and there is only a height deviation on the downstream side of the gap.

We applied our method to a schematic version of the flow through the Indonesian seas from the Pacific to the Indian Ocean. We used rules deduced from our theory to simplify the complex geometry. Numerical experiments suggest that the gravest two symmetric Rossby modes are important in the western boundary reflexion in the scenario of El Niños [*Battisti* 1988]. We found that $n = 1$ Rossby waves generate a reflected Kelvin wave with an amplitude of 85% of that which would be generated at a full boundary. For $n = 3$, it is above 74%.

Clarke [this issue] has carried out a similar calculation of the effects of the irregular geometry of the Western Pacific. He makes the same linear, long-wave modeling assumptions as are made here, and his paper provides some interesting justification for these crucial simplifications. His approach is also built on the work of *Cane and du Penhoat* [1982]; in fact, he makes more direct and elegant use of the island results of the earlier paper than we have done here. He makes somewhat different simplifications of the complex geometry of the region, but, reassuringly, the results are quite consistent with ours. Nonetheless, confidence in our mutual results must be limited by the recognition that both make the same important idealizations.

In carrying out a calculation as idealized as the one here, one hopes the results will be robust enough so that their possible application to the real world is obvious. We are not concerned with the details of the boundary flows, but did hope to deduce some general rules about the strength of the interior flow, i.e., the amplitude of the reflected Kelvin wave. As noted above, our results indicate some strong sensitivities to both the position of the gap and to the horizontal structure of the incoming flows. These remained even though we ignored nonlinearities and friction altogether and removed complexities one would expect from the highly irregular geometry of the western Pacific.

The complexity of the results from even such a simplified model convinces us that it will be difficult to be confident of any modeling study of the Indonesian flowthrough short of a highly resolved numerical calculation with a detailed representation of the geometry and bathymetry. Even then, uncertainties about the control exercised by the frictional parameterization will be hard to eliminate. Nonetheless, we offer a few tentative conclusions concerning the efficacy of the western equatorial Pacific "boundary" as a reflector.

The greatest sensitivity in our results concerns the region very near the equator. Since the western Pacific is effectively blocked within one to two radiis of deformation of the equator, low n Rossby modes will be largely reflected (Figures 1, 3; also cf. Figure 4). Thus if as proposed by *Zebiak* [1989] and *Battisti* [1989] among others, the reflections important for El Niño are primarily in motions well represented by the low-n Rossby modes, then this result suggests that the realistic boundary will not greatly alter expectations based on a simple solid boundary.

Further results (Figures 5, 6) suggest that if the incident motion is primarily poleward of the gap, then the reflection may be far less efficient than in the solid wall geometry. Thus for the Rossby waves incident north of 10°N emphasized by *White and Pazan* [1987] and *Graham and White* [1988] to be considered as actively initiating El Niño events, then some modification of our results will have to be offered.

As discussed in section 1, the observational evidence shows no anomalous flowthrough during El Niño events, lending support to the idea that the western end of the Pacific does act like a solid boundary. This is consistent with present results if the most important reflections are of motions in very low latitude, something which we believe on other grounds (see especially *Zebiak* [1989]).

Acknowledgments. Our thanks to Virginia DiBlasi for typing this difficult manuscript. Mark Cane was supported by NSF grant OCE8608386.

REFERENCES

Battisti, D. S. , Dynamics and thermodynamics of a warming event in a coupled tropical atmosphere-ocean model. *J. Atmos. Sci., 45*, 2889-2919, 1988.

Battisti, D.S., On the role of off-equatorial oceanic Rossby waves during ENSO. *J. Phys. Oceanogr., 19*, 551-559, 1989.

Cane, M.A., and Y. du Penhoat, On the effect of islands on low frequency equatorial motions. *J . Mar. Res., 40*, 937-962, 1982.

Cane, M.A., and P. Gent, Reflections of low-frequency equatorial waves at western boundaries. *J. Mar. Res., 42*, 487-502, 1984.

Cane, M.A., and E.S. Sarachik, Forced baroclinic ocean motions II; The linear equatorial bounded case. *J. Mar. Res., 35*, 395-432, 1977.

Cane, M.A., and E.S. Sarachik , Forced baroclinic ocean motion III; An enclosed ocean. *J. Mar. Res., 37*, 355-398, 1979.

Cane, M.A., and E.S. Sarachik, The response of a linear baroclinic equatorial ocean to periodic forcing. *J. Mar. Res., 39*, 651-693, 1981.

Clarke, A.J., On the reflection and transmission of low frequency engergy at the irregular western Pacific ocean boundary. *J. Geophys.. Res., this issue*

du Penhoat, Y., M.A. Cane, and R.J. Patton, Reflections of low frequency equatorial waves on partial boundaries. In *Hydrodynamics of the Equatorial Ocean, Memories Societe Royale des Sciences de Liege, Ser. 6, vol. 14, edited by* J.C.L. Nihoul, pp. 237-358, Elsevier, New York, 1983.

Graham, N.E., and W.B. White , The El Niño/Southern Oscillation as a natural oscillation of the tropical Pacific ocean/atmosphere system: Evidence from observations and models, *Science, 240*, 1293-1302, 1988.

Harrison, D.E., W.S. Kessler, and B.S. Giese, Ocean circulation model hindcasts of the 1982-83 El Niño: Thermal variability along ship of opportunity tracks. *J. Phys. Oceanogr., 19*, 397-418, 1989.

Lindstrom, E.R., et al., The Western Equatorial Pacific Ocean Circulation Study. *Nature, 330*, 533-537, 1987.

Lukas, R., Interannual fluctuations of the Mindanao current inferred from sea level. *J. Geophys. Res., 93*, 6744-6748, 1988.

McCalpin, J.D., A note on the reflection of low frequency equatorial Rossby waves from realistic western boundaries. *J. Phys. Oceanogr., 17*, 1944-1949, 1987.

Murray, S.P., and D. Arief, Throughflow into the Indian Ocean through the Lombok strait, January 1985 - January 1986. *Nature, 333*, 444-447, 1988.

Pazan, S.E., W.B. White, M. Inoue, and J.J. O'Brien, Off equatorial influence upon Pacific equatorial dynamic height variability during the 1982-1983 - El Niño/Southern Oscillation Event. *J. Geophys. Res., 91*, 8437-8449, 1986.

Piola, A.R., and A.L. Gordon, Pacific and Indian Ocean upper-layer salinity budget. *J. Phys. Oceanogr., 14*, 747-753, 1984.

White, W.B., and S.E. Pazan , Hindcast/forecasts of ENSO events based upon the redistribution of observed and model heat content in the western tropical Pacific, 1964-1986. *J. Phys. Oceanogr., 17*, 264-280, 1987.

White, W.B., G. Meyers, J.R. Donguy, and S. Pazan, Short-therm climatic variability in the thermal structure of the Pacific Ocean during 1979-1982. *J. Phys. Oceanogr., 15*, 917-935, 1985.

Wyrtki, K., *Physical Oceanography of the Southeast Asian waters. NAGA Rep. 2*, 195 pp., Univ. of Calif., Scripps Inst. Oceanogr. La Jolla, Calif., 1961.

Wyrtki, K., Indonesian through flow and the associated pressure gradient. *J. Geophys. Res., 92*, 12941-12946, 1987.

Zebiak, S.E., Oceanic heat content variability and El Niño cycles. *J. Phys. Oceanogr., 19*, 475-486, 1989.

Zebiak, S.E., M.A. Cane, A model El Ni o-Southern Oscillation. *Mon. Wea. Rev., 115*, 2262-2278, 1987.

M. Cane, Lamont-Doherty Geological Observatory of Columbia University, Palisades, NY 10964.

Y. du Penhoat, Groupe SURTROPAC (ORSTOM), Institut Français de Recherche Scientifique, Pour le Développement en Coopération, BP A5, Nouméa, New Caledonia.

(Received November 24, 1989;
revised June 8, 1990;
accepted June 14, 1990)